Fabrication and analysis of MEMS Test Structures for Residual Stress measurement

Akshdeep Sharma[*], Deepak Bansal[*], Maninder Kaur[*], Prem Kumar*, Dinesh Kumar[**] and K. J. Rangra[*]

[*]Sensors and Nanotechnology Group,Central Electronics Engineering Research Institute (CEERI), Council of Scientific and Industrial Research (CSIR), Pilani, Rajasthan, India,
akshdeepsharma@gmail.com, kjrangra@gmail.com
[**]Dept. of Electronics Science, Kurukshetra University, Kurukshetra, Haryana, India,
dineshelectronics@gmail.com

ABSTRACT

A set of test structures for in situ stress measurement is presented. The test structures were realized by means of surface micromachining, adopting photoresist as sacrificial layer and electroplated gold as structural layer. Initially array of buckling type test structures cantilevers, fixed-fixed beams, guckel rings and diamond were used to find out critical buckling beam. Later on rotational type pointer, double indicator and long-short beam strain sensor were analyzed to find out stress. Stress measurement techniques using micromachined structures are compared with the wafer curvature technique. Analytical calculations of the fabricated structures were performed for plated gold, the values of residual stress is found between 100 and 150MPa.

Keywords: MEMS test structures, residual stress, stress gradient, surface micromachining.

1 INTERODUCTION

In micro-electro-mechanical systems (MEMS) technology surface micromachining is widely used for creating thin film mechanical structures. There has been great interest in studying mechanical properties of thin films. The mechanical properties are very critical to the microstructure devices and can also influence the productivity and quality of these structures [1, 2]. One of the most important mechanical proprieties of thin films is the residual stress. Excessive compressive or tensile stress results in buckling, cracking, splintering and sticking problems. In particular, the residual stress is very important in MEMS applications and in cases where the thin film is designed to be a moving part. The mechanical displacement of the film is largely affected by the stress.

The investigation is concentrated on the development of two techniques buckling and rotation [3, 4]. The buckling technique is based on the buckling of a beam when exceeding a critical strain level. Therefore, an array with different beam lengths is required. The rotation technique, on the other hand, converts the extension or contraction of the material into a rotation, which can be easily measured. These structures have been modelled, simulated, fabricated and tested experimentally, using thin Au plated film. Both techniques have been shown to be promising methods for simple and accurate on-chip thin-film strain measurements. The results of stress calculation using each method are discussed and compared with conventional wafer curvature to calculate the average stress.

2 TEST STRUCTURES

Presently, it is very difficult to predict the residual stress from a growth process because the residual stress is strongly affected by deposition conditions and follows fabrication processes. Many techniques of stress measurement in thin films have been studied and proposed in the past several decades. The conventional method is measuring the wafer curvature to calculate the average stress using the Stoney's equation [5]. The stress can also be determined by nanoindentation technique [6]. The most popular and simplest method is the micromachining technique as it does not require special equipment and can be done by in situ measure.

The micromachining technique is the focus of this paper. Essentially, the test structure under stress is released after removing the underlying sacrificial layer. The structure will deform by increasing or decreasing the dimension of the structure because of the residual stress. The residual stress can thus be derived from this deformation. Several types of micromachining technique of stress measurement are described in detail as follows.

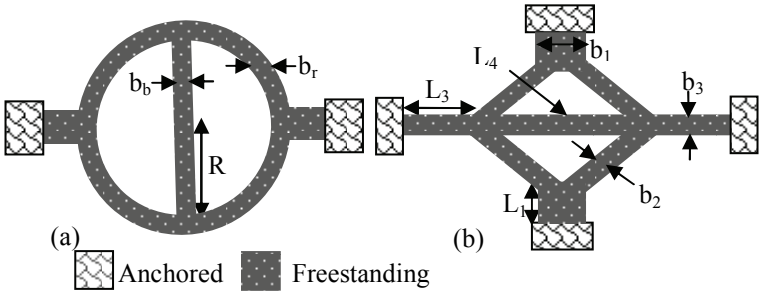

Figure 1. Stress measurement structures (a) Ring, (b) Diamond.

2.1 Buckling techniques

Stress in the thin film results in an extension or contraction of the released structure. This is basic principle of the stress measurement by buckling technique. The typical device normally used is a micro bridge. A micro bridge can only measure compressive stress. A micro bridge that is under compressive stress buckles after release. The stress can be expressed using critical buckled bridge dimensions as Eq.

$$\sigma = \frac{E}{1-\nu}\frac{\pi^2 h^2}{3L^2} \quad (1)$$

where E is the elastic modulus, ν is Poisson's ratio and E/(1−ν) is the biaxial modulus, L is the length of the critical buckled bridge, and h is the thickness of the bridge.

For tensile stress, the conversion structures shown in Fig. 1 are needed. The ring structure in Fig. 1(a) can be used to measure tensile stress only. If the freestanding structure is released, the ring deforms to an oval under tensile stress and the central beam becomes compressive. After removing the sacrificial layer in Fig. 1(b), the diagonal beams convert the tensile stress into compressive stress in the middle beam and the compressive stress causes the middle beam to buckle. On the other hand, the outside beams are buckling when the film stress is compressive stress [3]. Stress value can be derived from the maximum displacement of the central beam of a Guckel ring [6] as

$$\sigma = \frac{E}{1-\nu}\frac{0.515h^2}{R_c^2} \quad (2)$$

Where h is film thickness, R_c critical buckel radius.

2.2 Rotational techniques

The micromachined rotating structures as first presented by Drieenhuizen et al. [3] is shown in Fig. 2. The structure consists of two test beams and a rotating indicator beam. One end of each test beam is anchored to the substrate and the other is connected to the indicator. When the test beams are released by etching away the sacrificial layer, they are elongated or contracted due to the residual stresses. The test beams are slightly separated at the connection to the indicator beam, thus create a rotating deflection of the indicator beam. The deflection is directly proportional to the residual stress. Its direction corresponds to the type of stress, i.e. tensile or compressive stress. The residual stress can be calculated using Eq. 3, where LA, LB, W, O and δ are defined in Fig. 2(a).The CF is correction factor that consider the effect turning point width. The deflection of the indicator can be determined quite easily using an optical microscope or SEM.

$$\sigma = \frac{E}{1-\nu}\frac{O}{(L_A+L_B)(L_C+\frac{1}{2}O)}\frac{\delta}{CF} \quad (3)$$

One of the improved test structures is the double indicator structure shown in Fig 2(b) [3]. It can increase the sensitivity of the measurement by using two symmetrical structures as shown in Fig. 2(b). In this way, the double deflection can be measured. Under-etching and technology variations are eliminated. The stress can also be calculated using the Eq. (3).

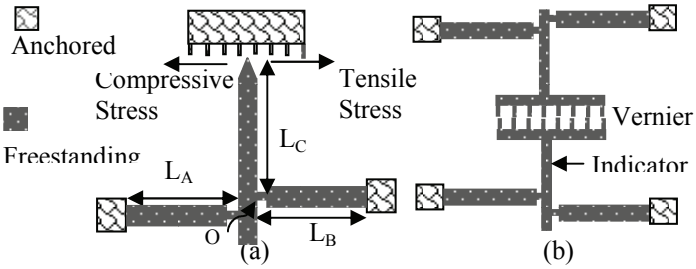

Figure 2. The schematic of rotating technique structure (a) pointer (b) Double indicator

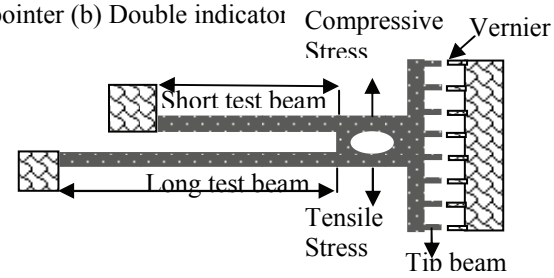

Figure 3. Schematic of the long–short beam strain sensor.

2.3 Long–short beam strain sensor

The long–short beam strain sensor is designed by Pan and Hsu [8]. Fig. 3 schematically shows the strain sensor. The sensor is comprised of a pair of long and short cantilever test beams with different lengths, long test beam and short test beam. The two beams are connected by a tip beam as an indicator. After the freestanding part is released, the two test beams will extend or contract due to residual stress in the thin film. The displacement (δ) caused by the deflection of two test beams can be read out using indicator and vernier by optical microscope or SEM. The stress is given by:

$$\sigma = \frac{E}{1-\nu}\gamma\delta \quad (4)$$

Where γ is the conversion factor related to geometrical parameters of the structure [7].This sensor can measure both tensile and compressive residual stress.

3 FABRICATION PROCESS STEPS

Fig. 4 shows the schematic view of fabrication process steps for test structures part of RF MEMS switch [9]. A set of microstructures were realized using surface micromachining techniques, on a 2″ diameter P-type <100> oriented silicon wafer. A thermal oxide was grown on the substrate, and then a conventional positive tone photoresist was deposited and patterned as a spacer layer. After that, the wafer was deposited with a chromium adhesion layer and gold seed layer by sputtering technique. Then a second photoresist was deposited and patterned, to work as a mould

for the electroplating structural layer 2 µm thick gold was plated by using a commercial sulphite bath solution. Wet etching methods were used to remove the photoresist mould and seed layer followed by a dry etching process to remove the sacrificial photoresist layer without generating stiction forces between membranes and the surface.

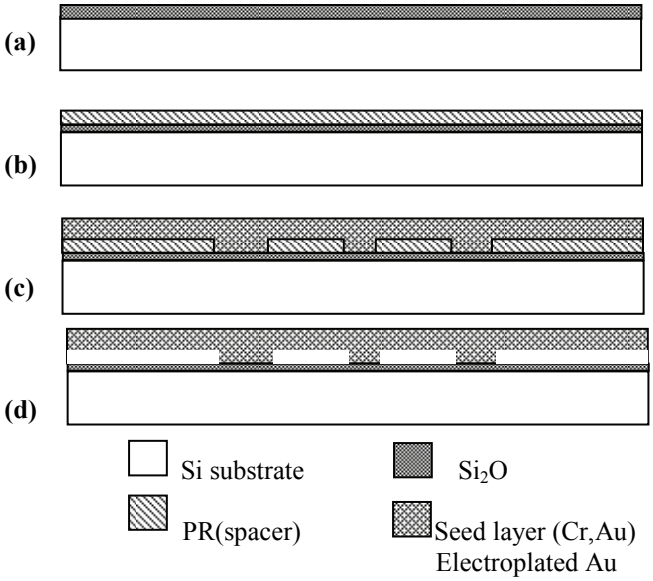

Figure 4. (a)-(d) Fabrication process steps for Test structures.

4 RESULTS AND DISCUSSION

Stress on thin films was investigated based on wafer curvature. Wafer curvature measurement is done by scanning the surface using profiler (AMBIOS XP-1). Silicon wafers are pre-stress by depositing a 1µm thick oxide using a wet oxidation process. Wafer curvature is measured before and after then electroplated Au thin film deposition. Due to the change in curvature after deposition, the intrinsic stress of the film can be deduced, using the Stoney's formula (Eq. 5). This equation yields a reasonable estimation of the stress in the thin film, considering the film thickness t_f much smaller than the substrate thickness t_s.

$$\sigma_f = \frac{E_s}{6(1-\nu_s)} \frac{t_s^2}{t_f} \left(\frac{1}{R_{sf}} - \frac{1}{R_f} \right) \quad (5)$$

where E_s and ν_s are respectively the substrate Young's modulus and Poisson's ratio, R_s and R_{sf} the measured curvature radii before and after film deposition. The accuracy of the film stress measurement is about 10%. A better accuracy can be obtained for small radius of curvature equivalent to highly stressed thin film. The measured average stress for 2µm thick electroplated gold is tensile 117.2MPa.

The total stress in a material is the sum of the mean residual stress and the stress gradient and can be written as:

$$\sigma_T = \sigma_0 + \sigma_G(y) \quad (6)$$

The stress gradient can be extracted from the deflection amplitude of different suspended cantilevers. When the structure is released, the stress gradient is calculated from the displacement amplitude.

$$\Delta\gamma = \frac{ML_{beam}^2}{2EI} = \frac{\gamma L_{beam}^2}{2} \quad (7)$$

The displacement at the edge of the cantilever is measured with an optical profiler (Veeco Wyko NT 9800), as shown in Fig. 5.

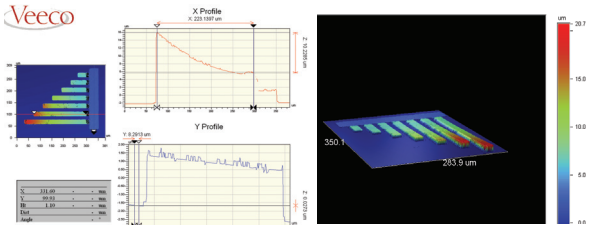

Figure 5. Optical profiler 2D,3D picture of 2µm thick and 20µm wide Au cantilevers, length ranging from 40-280µm.

The stress gradient $3.48\times10^{-4}\mu m^{-1}$ is extracted from the fit of the tip deflection versus the cantilever length curve in Fig. 6.

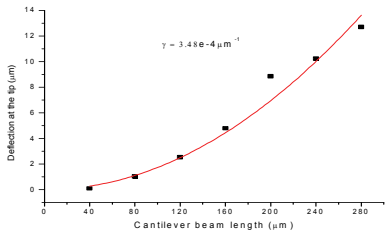

Figure 6. Measured deflection of the tip of cantilever presented in Fig. 5.

On chip test structures were designed to measure either compressive or tensile stress on the structural layer. According to wafer curvature measurement, a tensile stress was expected in the Au film and Guckel rings were fabricated to measure this stress. As shown in Fig.7, tensile stress tends to stretch the rings towards the anchors, inducing compressive moment on the central part. Stress value can be calculated from the ring dimensions for which buckling of the central part occurs. Stress value of the film can be derived from the maximum displacement of the central beam of the ring. The accuracy of this technique depends on the ability to find the closest set of rings for which small variation of beam length induces buckling, which is in this case for a ring inner diameter size between 110-120µm the two structures. The 3D optical profiler images of the ring array and SEM micrograph of critical buckle central beam of inner diameter 120µm are presented in Fig. 7. Accordingly calculated stress was 126.8, 106.5MPa for R_c 55, 60µm respectively. Considering the fact that the optimal ring for which the beam begins to buckle should be placed between the two rings. The

calculated stress value is in good agreement with the 117 MPa tensile stress measured using wafer curvature. The SEM micrographs of critical buckle diamond structure shown in Fig.8

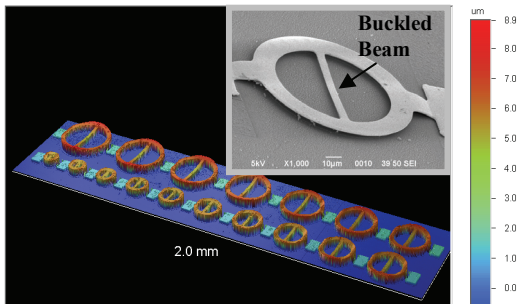

Figure 7. Optical profiler 3D picture 2µm thick Au Guckel rings array and SEM micrograph of ring with R_c 60µm.

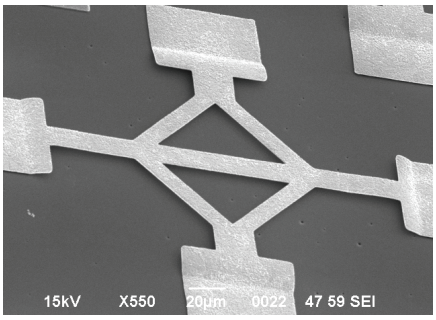

Figure 8. SEM micrograph of diamond ring strucures.

The pointer structure magnify tip deflection measured using SEM is shown in Fig. 9. This pointer displacement used for residual stress measuerment. Similar is the case with double indicator and long short beam strain sensor shown in Fig. 10 and 11 respectively.

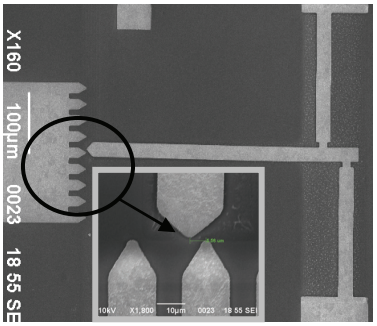

Figure 9. Pointer structures 2µm thick Au under tensile stress with vernier magnification

Several types of stress measurement methods including buckling technique, rotating technique, double indicator and long–short beam strain sensor have been reviewed. We have designed, fabricated and characterized the test structures for each method and results are shown in table1. The residual stress has in situ been measured for the same film by using different methods. It only requires a single significantly small structure size and can also be used for tensile and compressive stress. The double indicator structure is practically preferable for the stress monitoring because of its high reliability, easier calculation and higher accuracy.

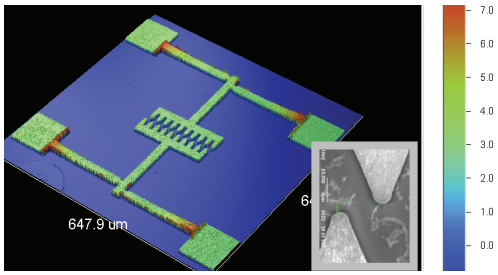

Figure 10. Double indicator structure under tensile stress with magnify SEM image for pointer displacement.

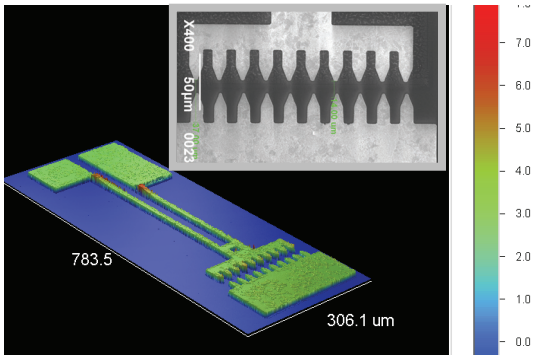

Figure 11. Long–short strain sensor under compressive stress in a 2 µm thick Au.

Table 1: Test results comparison of each stress test method

Stress test method	Measured displacement (µm)	Calculated stress (MPa)	FEA stress (MPa)
Cantilever	1-12	-	141
Ring structure	-	106.5,126.8	135
Diamond structure	0.385	-	134
Pointer structure	5.56	115.5	108
Double indicator structure	8.95	116.7	115
Long–short beam strain sensor	3.19	-	24

ACKNOWLEDGEMENTS

The authors would like to thank all the members of sensors and nanotechnology group for their help in fabrication of the devices and special thanks to NPL Delhi colleagues for providing optical profiler facility.

REFERENCES

[1] Y.J. Kim, M.G. Allen, IEEE Trans. Compon. Packag. Technol. 22, 282, 1999.

[2] L.Q. Chen, J.M. Miao, L. Guo, L.M. Lin, Surf. Coat. Technol.141, 96, 2001.
[3] B P van Drieenhuizen, Sensors and Actuators A, 37-38, 756-165, 1993.
[4] L. Elbrecht et. al, J. Micromech. Microeng. 7, 151–154, 1997.
[5] M.E. Thomas, M.P. Hartnett, J.E. McKay, J. Vac. Sci. Technol., A 6, 2570, 1988.
[6] S. Suresh, A.E. Giannakopoulos, Acta mater. 46, 5755, 1998.
[7] H. Guckel et. al, IEEE Trans. Electron Devices 35, 800, 1988.
[8] C.S. Pan, W. Hsu, J. Microelectromechanical Syst. 8, 200, 1999.
[9] K. Rangra et. al, Sensors and Actuators A, vol. 123-124, pp. 505-514, September 2005.